www.czasopisma.pan.pl PAN POLSKA AKADEMIA NAUK www.journals.pan.pl

A R C H I V E S O F M E T A L L U R G Y A N D M A T E R I A L S

Volume 56 2011 Issue 4

DOI: 10.2478/v10172-011-0104-y

W. PACHLA*, A. MAZUR*, J. SKIBA*, M. KULCZYK*, S. PRZYBYSZ*

EFFECT OF HYDROSTATIC EXTRUSION WITH BACK PRESSURE ON MECHANICAL PROPERTIES OF GREY AND NODULAR CAST IRONS

WPŁYW WYCISKANIA HYDROSTATYCZNEGO Z PRZECIWCIŚNIENIEM NA WŁASNOŚCI MECHANICZNE ŻELIWA SZAREGO I SFEROIDALNEGO

Cold hydrostatic extrusion with and without back pressure of ferritic-pearlitic grey cast iron EN-GJL 250 and ferritic-pearlitic nodular cast iron EN-GJS 500-7 has been performed. The experiments were performed on a originally designed hydrostatic extrusion press operating up to 2000 MPa with back pressure up to 700 MPa. Cast irons were cold hydrostatically extruded with back pressure in one pass with extrusion ratios up to 1.77 and 2.12 for grey and nodular one, respectively. Nodular cast iron was also successfully extruded without back pressure with extrusion ratio 1.35. Severe plastic deformation has led to axial alignment and elongation of graphite inclusions in extrusion direction together with sound flow of the surrounding metal matrix accommodating the strain without cracking. External high pressure has restrained of cracks generation and propagation during the material flow and healed of already existing defects by internal friction caused by plastic flow. It was visualized by aligned and elongated graphite flakes and nodules and no cracks and porosity observed in surrounded metal matrix. Very high compressive strength of both materials has been measured, above 1000 MPa and ~2400 MPa for grey and nodular cast iron, respectively. These values were accompanied by above 3000 MPa and above 3400 MPa microhardnes HV0.2 and by over 15% and over 50% elongation at maximum strength for those materials, respectively. Cast irons with such properties can be classified as a new iron-base structural materials.

Keywords: hydrostatic extrusion; back pressure; severe plastic deformation; graphite; cast iron; mechanical properties

Procesowi wyciskania hydrostatycznego na zimno poddano ferrytyczno-perlityczne żeliwa szare EN-GJL 250 i sferoidalne EN-GJS 500-7. Eksperymenty prowadzono na oryginalnej, własnej konstrukcji prasie do wyciskania hydrostatycznego pracującej do 2000 MPa z przeciwciśnieniem do 700 MPa. Żeliwa były wyciskane z sukcesem z przeciwciśnieniem w jednej operacji ze stopniem redukcji 1.77 i 2.12 odpowiednio, dla żeliwa szarego i sferoidalnego. Żeliwo sferoidalne było również wyciskane bez przeciwciśnienia ze stopniem redukcji 1.35. Duże odkształcenie plastyczne prowadziło do osiowego ułożenia i wydłużenia wtrąceń grafitu w kierunku wyciskania przy jednoczesnym płynięciu metalowej osnowy zapewniającej odkształcenie bez pęknięć. Wysokie ciśnienie przyłożone na zewnątrz odkształcanego produktu powtrzymywało generowanie i propagację pęknięć podczas płynięcia materiału oraz 'leczyło' istniejace już defekty wewnętrzne poprzez zgrzewanie tarciowe podczas odkształcenia plastycznego. Uwidaczniały to ułożone i wydłużone w kierunku wyciskania płatki i kulki grafitu oraz brak pęknięć i porowatości obserwowany w otaczającej je osnowie. Zmierzono bardzo wysoką wytrzymałość na ściskanie obu materiałów, ponad 1000 MPa i ok. 2400 MPa, odpowiednio dla żeliwa szarego i sferoidalnego. Wartościom tym towarzyszyła mikrotwardość HV0.2 powyżej 3000 MPa i powyżej 3400 MPa oraz ponad 15% i ponad 50% wydłużenie przy maksymalnej wytrzymałości, odpowiednio dla obu tych materiałów. Żeliwa o takich własnościach można kwalifikować jako nowe materiały konstrukcyjne na bazie żelaza.

1. Introduction

The properties of cast iron depend to a great extend on the morphology, amount and anisotropy of the graphite phase. Graphite flakes with random orientation present in grey cast iron limit its application for many years. It is due to its low tensile strength and low ductility. Therefore, some methods to control graphite morphology as modification, spheroiding treatment and alloying have been developed [1, 2]. The plastic deformation as the reason of the strength improvement in cast irons have been related mainly to high temperature processing and reported occasionally [3-6]. It is understandable when brittleness and difficulty in obtaining products without cracks, especially of grey cast iron, is taken into account. On the other hand, hot deformation

* INSTITUTE OF HIGH PRESSURE PHYSICS, POLISH ACADEMY OF SCIENCES (UNIPRESS), 01-142 WARSZAWA, 29 SOKOLOWSKA STR., POLAND

involves the main disadvantage, the thermal softening effects which restricts of strength level possible to obtain. Therefore, any solution involving the cold deformation processing of cast irons would be preferable when the high-strength iron is the main goal which is considered. Only, one paper [7] describing deformation in cold condition such as the upset forging of globular cast iron have been found out throughout the last years literature survey. True strain of ~0.38 in sound compressed products after special melt treatment and graphitizing were obtained. Higher degrees of deformation have required steel holders with 7.5 mm wall thickness. Application of grey cast iron, due to its low strength and trace quantities of ductility caused by randomly distributed graphite flakes, is very limited. In a very exceptional paper on plastic deformation of grey cast iron, hot compression at 900°C in steel cylinder has enable to achieve true strain ~1.6 [3]. Graphite flakes were aligned normally to compression direction with some flakes adhered to each other. Special ferritizing treatment applied after deformation doubled tensile strength up to ~250 MPa in comparison to state before compression [3].

First attempts to apply back pressure to extrusion of cast irons were done at the beginning of sixties of last century by Pugh and Low [8] and Bulychev and Beresnev [9]. The benefits of back pressure application have been demonstrated by extrusion of one of the grey cast iron grades (EN-GJL-200), however, achieved result was not very spectacular and description of the experimental conditions very brief [10]. Since then, no study of application of hydrostatic extrusion to deformation of cast irons have been reported.

In present paper improvement of mechanical properties in grey and ductile (nodular) cast irons processed by severe plastic deformation (SPD) in cold condition is undertaken. Unique process of hydrostatic extrusion with back pressure is applied. Hydrostatic back pressure was successfully applied for the first time between 1958-1963 for conventional extrusion of bismuth, magnesium and brass and presented by Pugh, Green and Gunn [11, 12]. It was shown, that for selected brittle materials back pressure imposed on exiting products restrain their fracture by lowering tensile stresses in processed materials below the critical stresses necessary to crack initiation and propagation.

2. Experimental procedure

The materials studied were commercially offered laminar ferritic-pearlitic grey cast iron EN-GJL 250 (GCI) and ferritic-pearlitic nodular (ductile) cast iron EN-GJS 500-7 (NCI), which chemical compositions are shown in Table 1. Both materials were supplied in the form of cast ingots with an outer diameter of 30 mm. Ingots were machined to form the extrusion billets between 7 mm and 17.5 mm in OD and hydrostatically extruded (HE) without and with back pressure (BP) into rods between 4 mm and 16 mm in OD. Extrusion experiments were carried out at Unipress press operating up to 2000 MPa with back pressure up to 700 MPa. All tests were carried out at room temperature with die angles 18°, 30° or 45° and back pressures of 400 MPa, 500 MPa or 700 MPa, each time selected individually. A lubricant paste based on ~60% MoS_2 and refined oil was used. The tests were often repeated to adapt the best process parameters (extrusion speed, billet nose geometry, die angle, etc.). Experiments were made with linear extrusion speed varied between 0.3 m/min and 2.5 m/min which corresponds to strain rates between 1.1 s^{-1} and 3.2 s^{-1}.

TABLE 1

Chemical composition of tested cast irons (wt.%)

	C	Si	Mn	S	P	Cr	Mg
grey cast iron GCI	2.70	1.71	0.73	0.028	0.03	0.055	–
nodular cast iron NCI	3.31	2.42	0.164	0.01	0.027	0.014	0.042

The optical profilometer Hommel tester T8000 was used to investigate the surface quality of selected initial billets and extruded rods. The structures were examined using an optical microscope Nikon Eclipse LV150. The initial and as-extruded samples were examined on polished and etched longitudinal and transverse cross-sections. Microhardness was measured on the transverse and longitudinal sections of the extruded rods after disc cutting or trimming and polishing on a HV automated Zwick/Roell ZHV microhardness tester with load of 200 g and a 15 s test period. Statistical approximations was carried out to estimate the mean value of microhardness HV and the coefficient of variation CV(HV) defined as the ratio of the standard deviation of HV, i.e.: SD(HV) to its mean value HV. Static tensile and compression tests were made on a Zwick/Roell Z250kN machine in room temperature and at a constant strain rate of $0.008s^{-1}$ with fivefold (tension) and one and half times (compression) specimens. The tested specimen were machined from the as-extruded products.

3. Results and discussion

The pressure characteristics of hydrostatic extrusion without and with back pressure for grey cast iron (GCI) and nodular cast iron (NCI) are shown in Fig. 1. They reflect general tendency observed for other materials [10] of an increase of extrusion pressure with increasing true strain defined as natural logarithm of extrusion ratio R, where extrusion ratio reflects the ratio of billet to product

cross sections. The presented chart includes also points of failed experiments, where disintegrated (cracked) or with a poor quality surface products have been obtained.

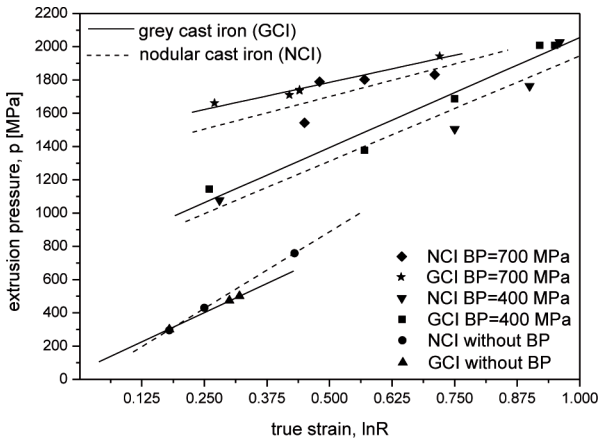

Fig. 1. The pressure characteristics of hydrostatic extrusion without and with back pressure for grey cast iron (GCI) and nodular cast iron (NCI)

These points serve only for rough estimation of the extrusion pressure trend for each material. For this same true strain the extrusion pressure is higher for GCI than for NCI and it is also higher for higher back pressure applied.

The GCI was not extruded successfully without back pressure, while for NCI only the small extrusion ratio R=1.36 (true strain ε=0.31) was possible. The maximum strains available for each material to obtain uncracked, sound products during hydrostatic extrusion with and without back pressure are given in Table 2, and the related products are shown in Fig. 2.

The application of back pressure has enabled to extrude uncracked GCI products and has extended available strains for uncracked NCI one, Fig. 2. It is believed, that current results for GCI are the first reported since the precursory work done by Pugh and Low in 1964 [8], where authors have reported hydrostatic extrusion with back pressure of grey cast iron EN-GJL-200, although in very short product does not exceeding four times its diameter obtained with extrusion ratio R=3 and back

TABLE 2
Maximum strains at which the sound products were obtained during cold hydrostatic extrusion of cast iron

Material	Without back pressure		With back pressure	
	Extrusion ratio, R	True strain, ε	Extrusion ratio, R	True strain, ε
GCI	–	–	1.77	0.57
NCI	1.35	0.30	2.12	0.75

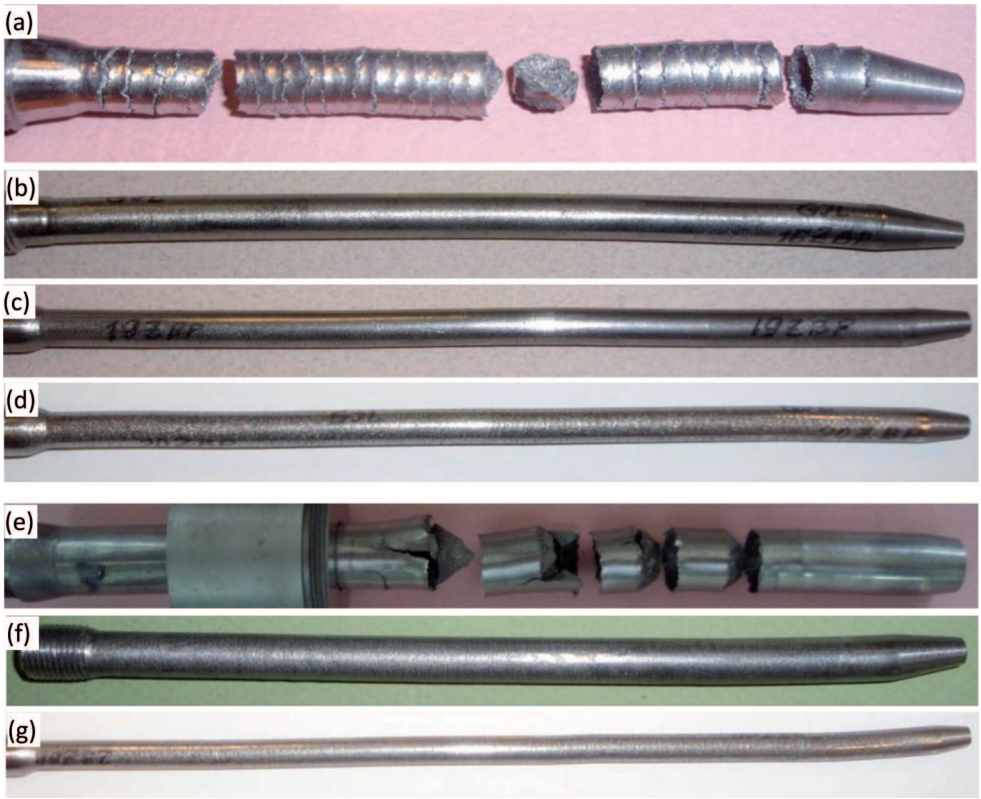

Fig. 2. Images of hydrostatically extruded grey cast iron (GCI) products (a)-(d) and nodular cast iron (NCI) products (e)-(f); (a) and (e) – without back pressure, the rest – with back pressure; (a) GCI, extrusion ratio R=1.35 (true strain ε=0.3), (b) GCI, R=1.31 (ε=0.27), (c) GCI, R=1.77 (ε=0.57), (d) GCI, R=2.11 (ε=0.75), and (e) NCI, R=1.56 (ε=0.46), (f) NCI, R=1.56 (ε=0.46) i (g) NCI, R=2.12 (ε=0.75)

pressure of 635 MPa. According to pressure characteristic obtained in current work extrusion ratio of R=3 would involve extrusion pressure of ~2200 MPa, i.e.: much higher than that reported in Ref.[8] of 1630 MPa. However, extrusion ratio R=3 was not achieved during present experiments, what can results from approx. 25% stronger and 27% harder grey cast iron grade applied in current work.

This strain increase caused by application of back pressure was almost one and a half times for NCI. An indisputable, beneficial effect of back pressure on the product's integrity during cold hydrostatic extrusion was observed, however, not always the quality of product surfaces were acceptable. Surface defects have been observed in both extruded products with and without back pressure, Fig. 3. This defect is commonly observed during deformation through conical converging die of the hard and brittle materials and is commonly called 'fir tree' or 'fish skin' defect [13]. The intensity of surface defects appearance has increased with an increase of extrusion ratio but it did not affected the high strength properties within the product interior. For this same extrusion ratio the more brittle grey cast iron was much more susceptible for development of surface defects in comparison to nodular one.

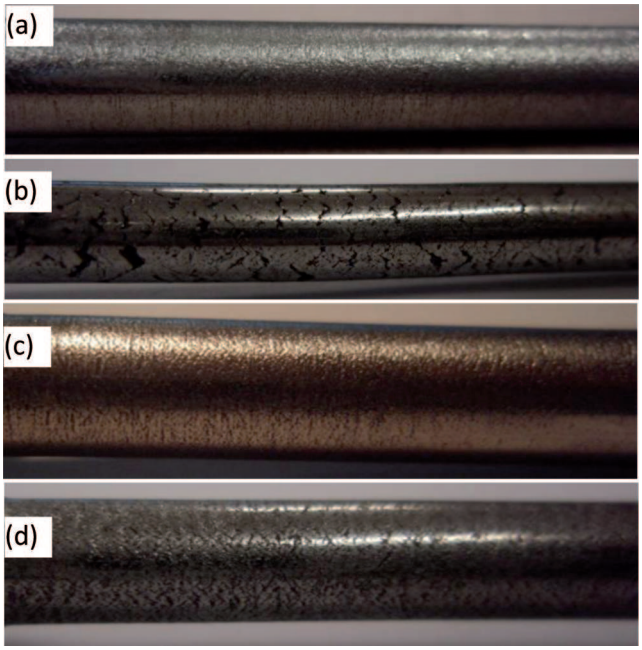

Fig. 3. Surface cracking defects ('fir tree') during hydrostatic extrusion with back pressure of (a) grey CI, extrusion ratio R=1.31 (true strain ε=0.27), (b) grey CI, R=2.59 (ε=0.95), (c) nodular CI, R=1.32 (ε=0.28), and (d) nodular CI, R=2.12 (ε=0.75)

The longitudinal surface roughness of billet material (after machining) was twice smaller, Ra=1.5μm vs. 3μm, for GCI in comparison to NCI. After extrusion the surface roughness of products for both materials was getting worse maintaining still higher values of Ra for NCI, Fig. 4. This resulted from the 'fir tree' effect intensification caused by more severe plastic deformation. Tendency of worsening the surface roughness with an increase of strain was observed. The surface quality (longitudinal roughness values) of the extruded GCI products varied between Ra = 2-4 μm and for the NCI products between Ra = 2.5-6 μm. Higher deterioration in NCI resulted from higher starting billet roughness and higher extrusion ratios applied.

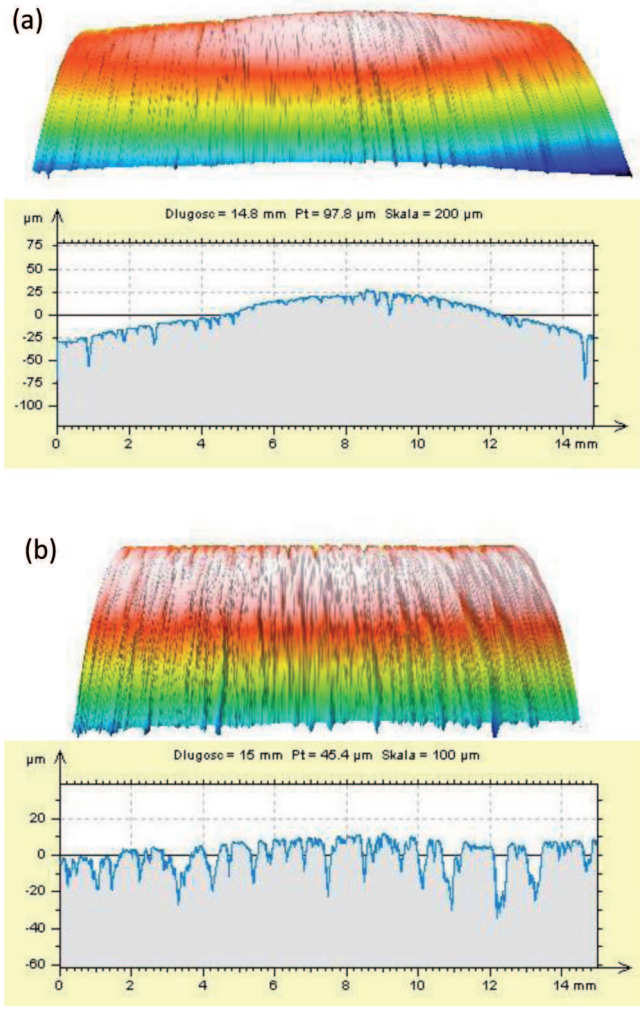

Fig. 4. Surface roughness after hydrostatic extrusion with back pressure of 500 MPa (a) grey cast iron EN-GJL 250 with extrusion ratio of R=1.77 (true strain ε=0.57), and (b) nodular cast iron EN-GJS 500-7 with extrusion ratio of R=2.12 (true strain ε=0.75).

The application of back pressure has enabled to apply severe plastic deformation in one extrusion pass and to achieve sound (uncracked) products with evidently elongated microstructure, Fig. 5. Comparison either graphite flakes spatial distribution, Fig.5 (a), either shapes of graphite nodules, Fig. 5 (c), with their random distribution and circular shape in starting billet materials confirms the axial alignment and elongation of graphite inclusions in extrusion direction together with flow of

the surrounding metal matrix around which accommodates the strain without cracking. No voids or residual porosity were observed in extruded products. For better visualization of microstructure alignment the graphite morphology in transverse sections of extruded products are presented in Fig. 5 (b) and (d). Random distribution of graphite flakes and equiaxed nodular shapes in transverse sections confirms longitudinal structure alignment.

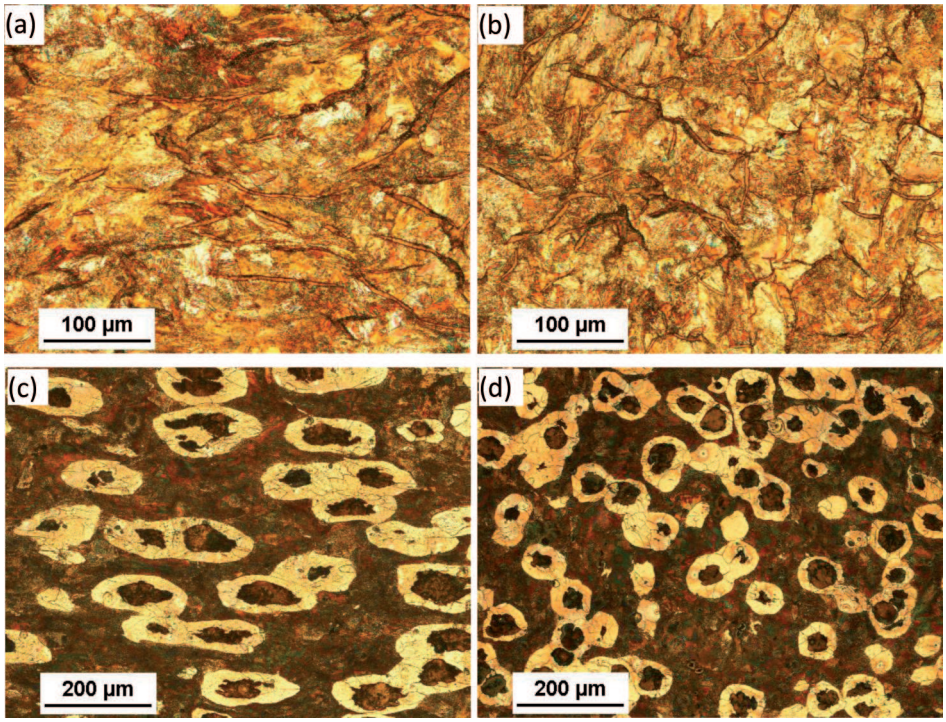

Fig. 5. Morphology of graphite flakes and nodules alignment and shape in (a), (b) grey cast iron GCI and (c), (d) nodular cast iron NCI after cold hydrostatic extrusion with back pressure with extrusion ratio R=1.6 (true strain ε=0.47); (a) and (c) longitudinal section, (b) and (d) transverse section; Note: extrusion direction horizontal, parallel to the image base

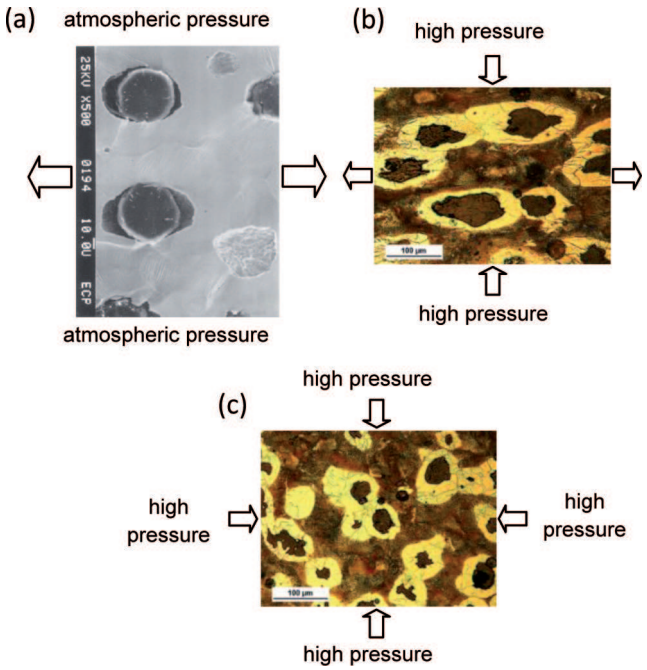

Fig. 6. Deformation at atmospheric pressure (a) vs. deformation under pressure (b), (c) for nodular cast iron; (a) from [15] tensile test of EN-GJS-400 cast iron, (b) hydrostatic extrusion of EN-GJS-500 cast iron with extrusion ratio of R=1.56 (true strain ε=0.45) to back pressure of 740 MPa, longitudinal section, (c) transverse section

Fig. 6 explains the reason why hydrostatic extrusion increases strain to fracture and shows the beneficial role of back pressure superimposed on the extruded product. During tensile stresses imposed on NCI at atmospheric pressure first, the shear bands at sites where the local yield stress was reached, emanating from the equator of nodules due to the localization of matrix plastic deformation are observed [14]. With strain continuing decohesions at the poles of the nodules oriented in direction of applied stress occur and the voids growing in stress direction are formed, Fig. 6(a) [15]. Finally, the transverse to stress direction failure occurs due to matrix decohesions at nodules equator and linkages of adjacent voids. Contrary to this situation, during hydrostatic extrusion with back pressure, on material within the deformation zone in extrusion die the tensile stresses in extrusion direction and two-axial circumferential compressive stresses are acting, followed by pure hydrostatic state of stresses acting on the emerged product in the back pressure chamber. This causes, that the decohesion stages at graphite nodule/metal matrix interface are shifted towards the higher strains what significantly increases elongation to failure, Fig. 6(b) and (c). Material consistency due to privileged state of stresses is enhanced. Graphite nodules show tensile elongation in extrusion direction, Fig. 6 (b) remaining circular in perpendicular direction, Fig. 6 (c) without any decohesions at the matrix/nodules interfaces. Due to increased density and extended ductility both, GCI and NCI can be deformed to sound products, see Table 2 and Fig. 3. Similar decohesion suppressing occurs at graphite flakes interface in grey cast iron. However, since the stress concentration is more intense at the tips of the graphite flakes edges due to the micronotch stress concentration, the 'pressure induced ductility' effect is smaller for GCI iron in comparison to NCI. Thus, the available sound strains are also lower.

Influence of high hydrostatic pressure on brittle material is twofold. The first is to restrain of cracks generation and propagation during the material flow. But there is the second, equally important factor, i.e.: healing of already existing defects as voids, cavities, interface decohesions, etc. by shear bonding of existing interfaces during internal friction caused by plastic flow. This increases the material integrity, thus density and is also responsible for enhancement of material sound flow. Both factors act parallel during hydrostatic extrusion with back pressure and that's why application of back pressure in case of NCI has allowed for 2.5 fold increase of true strain in comparison to hydrostatic extrusion without BP, Table 2.

In Fig. 7 compression strength, yield stress at compression and elongation at maximum strength for GCI (a) and NCI (b) after cold hydrostatic extrusion with back pressure are shown. Values for initial as-cast material and material cited in standards are also given. Both cast irons show evident increase of yield stress at compression $\sigma_{d0.2}$ after deformation (extrusion), moderate for GCI by maximum 13%, Fig. 7(a), and strong increase for NCI, Fig. 7(b) by ~50% in comparison with initial material. Compression strength σ_{dM} behaves differently, for GCI increasing up to ~20% and then, at maximum true strain ε=0.57 showing abrupt drop down by –6%, and for NCI showing permanent increase by ~40% at maximum. This various response in case of σ_{dM} can results from higher stress concentration generated during compression of flake graphite GCI thus more spontaneous fracture generation and propagation in this cast iron. It is confirmed by over 50% drop in elongation at maximum strength ε_{dM} for GCI, while for NCI elongation shows continuous improvement with an increase of true strain at the level similar to $\sigma_{d0.2}$, Fig. 7(b).

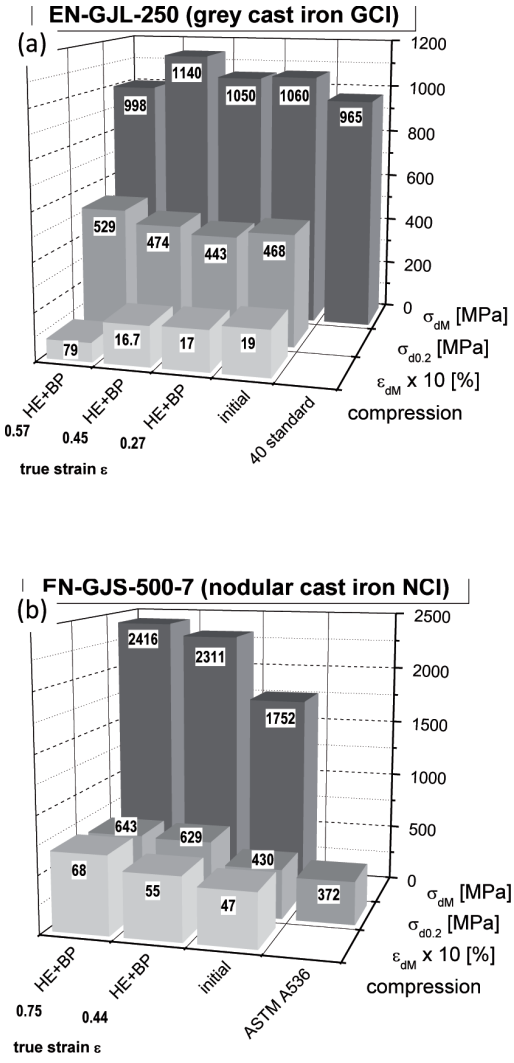

Fig. 7. Compression strength, yield stress at compression and elongation at maximum strength for (a) grey cast iron GCI and (b) nodular cast iron NCI after cold hydrostatic extrusion with back pressure

In Fig. 8 microhardness HV0.2 for GCI (a) and NCI (b) after cold hydrostatic extrusion with back pressure are shown. For GCI increase in hardness is even higher, by ~30% than an increase in strength (by less than 20%), Fig. 8(a). It is understandable when higher density of internal defects for grey cast iron is considered. Increase in density is associated with an improvement in hardness distribution, i.e. coefficient of variation CV(HV) decreases. When true strain approaches maximum available value at which still 'sound' product is obtained, decrease of σ_{dM} and HV0.2 with adequate increase of CV(HV) are observed. It suggests that the process of microcracks generations is already initiated, Fig. 7(a) and 8(a).

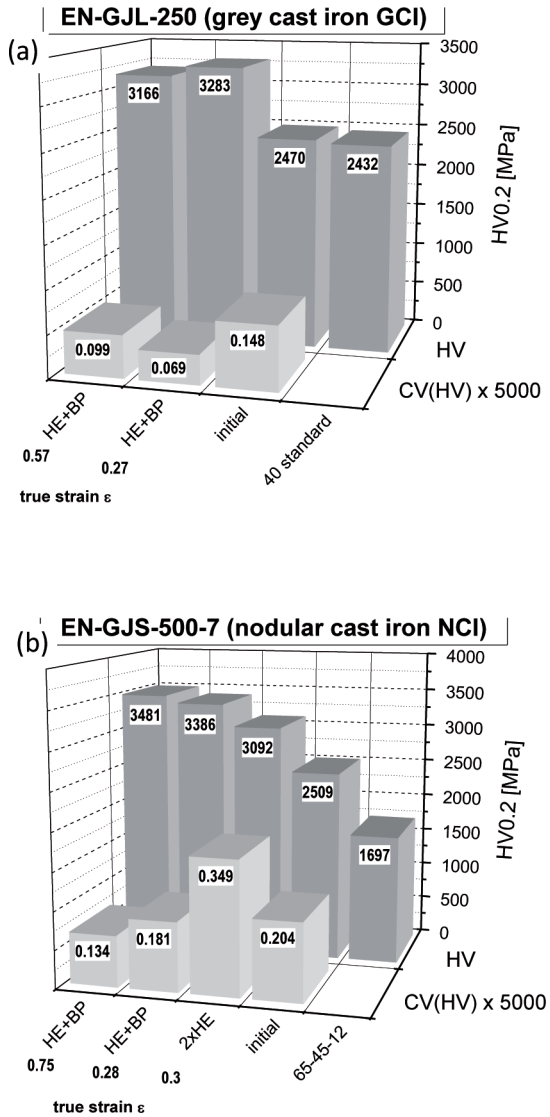

Fig. 8. Microhardness HV0.2 for (a) grey cast iron GCI and (b) nodular cast iron NCI after cold hydrostatic extrusion with back pressure

Nodular cast iron (NCI) shows continuous increase of HV0.2 up to maximum 40% with an increase of true strain for all sound flow products, Fig. 8(b). It is accompanied with progressive CV(HV) decrease what indicates, that the density distribution is continuously improved. It should be noticed, that this same true strain achieved without and with back pressure, leads to twice lower CV(HV) and simultaneously by 10% higher HV for the last, what would suggests that use of back pressure substantially improves density and homogeneity of extruded product, Fig. 8(b).

There is no literature data on cold deformation of GCI and very seldom as Ref. [7] for NCI. For a very brittle materials such as cast irons only hot deformation methods, as hot compression and hot rolling have been successfully applied [3-7]. Deformation temperatures are high, usually between 900-1050°C, occasionally drop to 600°C [4]. Lower temperatures are related to low true strains, while highest true strains are available at temperatures ~900-1000°C. This is not really economical way of run plastic deformation, especially when the resulting mechanical properties are not very challenging. In Table 3 comparison between mechanical properties of grey cast irons (GCI) and nodular cast irons (NCI) deformed by traditional hot deformation methods and deformed by cold hydrostatic extrusion with back pressure are presented. It is seen, that threefold lower true strain applied by hydrostatic extrusion with back pressure increases ultimate strength of GCI over 4 times and hardness by ~40% with 2-3 fold increase of deformation to fracture in comparison to hot deformation at atmospheric pressure. Similar tendencies are observed for NCI, where over twofold increase of ultimate strength and fifteen times increase in deformation to fracture are observed, Table 3. This drastic increase in ultimate strength and deformation to fracture is associated with ~25% drop in yield stress for GCI iron.

Such improvement in mechanical properties of cast irons could be obtained due to the hydrostatic state of stresses imposed on deformed products which has increased materials density, healed origin defects (microcracks and voids) and improved material consistency thus has allowed to increase deformation to fracture at room temperature. Increase in ultimate strength is higher for GCI iron than for the NCI one, what is associated with higher degree of strain hardening observed in GCI than in NCI [16]. It is due to the lower level of stress concentration introduced by graphite nodules in comparison to graphite flakes, thus higher strains available for NCI resulting in higher strength and hardness after deformation.

TABLE 3

Comparison between mechanical properties of grey cast irons (GCI) and nodular cast irons (NCI) deformed by traditional methods and deformed by hydrostatic extrusion with back pressure (most data obtained in compression tests)

Material	Deformation and sample preparation	True strain ε	UTS MPa	YS MPa	El %	HV MPa	Ref.
GCI	Hot compression 900°C + ferritizing treatment [(a)]	1.61	249		5.2	2130	[9]
	HE + BP[(b)]	0.45	1140	474	17	2800	current
	HE + BP	0.57	998	529	8	3170	current
NCI	Hot compression 600-950°C	0.25	725				[11]
	Cold upset (forging)	0.51	850				[10]
	Hot deformation	1.61	1060	850	4.5		[13]
	Hot rolling 900-1050°C + normalization [(a)]	2.53	1030	840	5.5		[12]
	HE + BP	0.44	2310	630	55	3240	current
	HE + BP	0.75	2410	643	68	3480	current

[(a)] tensile properties

[(b)] HE+BP – hydrostatic extrusion with back pressure

4. Conclusions

For the first time systematic studies of cold plastic deformation of grey and nodular cast irons has been performed. It was possible due to application of unique method of hydrostatic extrusion combined with back pressure. It has allowed to gain not available by any other methods level of compression strength, σ_{dM} and yield stress at compression $\sigma_{d0.2}$ in grey cast iron, >1000 MPa and ~500 MPa, respectively, and in nodular cast iron ~2400 MPa and >600 MPa, respectively. These properties were accompanied by >15% and >50% elongation at maximum strength ε_{dM} and >3000 MPa and >3400 MPa microhardnes HV0.2 for GCI and NCI, respectively. Obtaining of extreme high properties was possible due to cold deformation with adequate high strains resulting in sound, uncracked products. It was able due to hydrostatic state of stresses superimposed on material during plastic deformation. Cast irons with such properties can be classified as a new iron-base structural materials in the range of applications as electrode wires, gears, milling bodies, etc., knowing, that corrosion resistance of deformed cast iron is higher than those of cast iron [17].

Acknowledgements

This work was conducted within the grant No. R15 033 02 awarded by the Polish Ministry of Science and Higher Education. The authors are grateful to K. Wojciechowski and M. Przybysz from Institute of High Pressure Physics, Polish Academy of Sciences for assistance in high pressure experiments.

REFERENCES

[1] L. Haenny, G. Zambelli, The stiffness and modulus of elasticity of grey cast irons, J Mater Sci Lett **2**, 239-242 (1983).

[2] M. Ramadan, M. Takita, H. Nomura, Effect of semi-solid processing on solidification microstructure and mechanical properties of gray cast iron, Mater Sci Engin A **417**, 166-173 (2006).

[3] W. Wei, J. Tianfu, G. Yuwei, Q. Guiying, Z. Xin, Properties of gray cast iron with oriented graphite flakes, J Mater Proces Technol **182**, 593-597 (2007).

[4] K. Qi, F. Yu, F. Bai, Z. Yan, Z. Wang, T. Li, Research on the hot deformation behaviour and graphite morphology of spheroidal graphite cast iron at high strain rate, Materials and Design **30**, 4511-4515 (2009).

[5] N.P. Lyakishev, G.V. Shcherbedinskii, Hot plastic deformation of high-strength cast iron, Metal Science and Heat Treatment **43**, 421-422 (2001).

[6] V. Shumikhin, Deformed ductile cast-iron. Science and Innovation, special issue 2007; p.104, www.atsukr.org.ua.

[7] J. Baca, A.S. Chaus, Effect of plastic deformation on the structure and properties of cast iron with globular graphite, Metal Science and Heat Treatment **46**, 188-191 (2004).

[8] H.Ll.D. Pugh, A.H. Low, J. Inst Metals **93**, 201 (1964).

[9] D.K. Bulychev, B.I. Beresnev, Fiz. Metal. Metalloved **13**, 942 (1962).

[10] H.Ll.D. Pugh, The application of hydrostatic pressure to the forming of metals. In: H.Ll.D. Pugh, editor. Mechanical behaviour of materials under pressure, Amsterdam: Elsevier Publ Co Ltd; p.522-590 (1970).

[11] H.Ll.D. Pugh, D. Green, Progress Report on the behaviour of materials under hydrostatic pressure, MERL

Plasticity Report No 147, National Engineering Laboratory, East Kilbride, Glasgow (1958).

[12] H.Ll.D. P u g h, D. G u n n, Symposium on the physics and chemistry of high pressures, Society of Chemical Industry, London, p.157-162 (1963).

[13] B. A v i t z u r, Handbook of Metal-forming Processes. New York: John Wiley & Sons Inc; p.103 (1983).

[14] M.J. D o n g, C. P r i o u l, D. F r a n c o i s, Damage effect on the fracture toughness of nodular cast iron: Part I. Damage characterization and plastic flow stress modelling, Metall Mater Tran A, **28A**, 2245-2254 (1997).

[15] T. S e i f e r t, H. R i e d e l, Mechanism-based thermomechanical fatique life prediction of cast iron. Part I: Models, Int J Fatique **32**, 1358-1367 (2010).

[16] T o r s t e n S j ö g r e n at liu.diva-portal.org/smash /get/diva2:23475/FULLTEXT01.

[17] G.V. S h c h e r b e d i n s k i i, Iron: promising material of the XXI century, Metal Science and Heat Treatment **47**, 333-342 (2005).

Received: 20 April 2011.